

H. PAUL\*, P. ULIASZ\*\*, M. MISZCZYK\*, W. SKUZA\*, T. KNYCH\*\*

## AN SEM/EBSD STUDY OF SHEAR BANDS FORMATION IN Al-0.23%wt.Zr ALLOY DEFORMED IN PLANE STRAIN COMPRESSION

### KRYSTALOGRAFICZNE ASPEKTY FORMOWANIA SIĘ PASM ŚCINANIA W STOPIE Al-0.23% wag.Zr ODKSZTAŁCANYM W PRÓBIE NIESWOBODNEGO ŚCISKANIA

The crystal lattice rotations induced by shear bands formation have been examined in order to investigate the influence of grain boundaries on slip propagation and the resulting texture evolution. The issue was analysed on Al-0.23wt.%Zr alloy as a representative of face centered cubic metals with medium-to-high stacking fault energy. After solidification, the microstructure of the alloy was composed of flat, twin-oriented, large grains. The samples were cut-off from the as-cast ingot in such a way that the twinning planes were situated almost parallel to the compression plane. The samples were then deformed at 77K in channel-die up to strains of 0.69. To correlate the substructure with the slip patterns, the deformed specimens were examined by SEM equipped with a field emission gun and electron backscattered diffraction facilities.

Microtexture measurements showed that strictly defined crystal lattice re-orientations occurred in the sample volumes situated within the area of the broad macroscopic shear bands (MSB), although the grains initially had quite different crystallographic orientations. Independently of the grain orientation, their crystal lattice rotated in such a way that one of the {111} slip planes became nearly parallel to the plane of maximum shear. This facilitates the slip propagation across the grain boundaries along the shear direction without any visible variation in the slip plane. A natural consequence of this rotation is the formation of specific MSB microtextures which facilitates slip propagation across grain boundaries.

**Keywords:** Shear bands, Texture, Microstructure, Electron diffraction, Low temperature deformation

W pracy analizowano wpływ rotacji sieci krystalicznej wywołanej pojawieniem się pasm ścinania na propagację poślizgu poprzez granice ziaren oraz na ewolucję tekstury. Badania prowadzono na próbkach stopu Al-0.23%wag.Zr, jako reprezentatywnym dla grupy metali o średniej i dużej energii błędu ułożenia. W stanie wyjściowym w mikrostrukturze stopu dominowały duże, silnie spłaszczone ziarna, bliźniaczo względem siebie zorientowane. Z odlanego wlewka wycinano próbki w ten sposób, że płaszczyzny zbliźniczenia usytuowane były równoległe do płaszczyzny ściskania. Badania zachowania umocnieniowego analizowano w próbie nieswobodnego ściskania prowadzonej w temperaturze 77K. Próbkę odkształcano do zakresu ~50% zgniotu. Analizę zmian strukturalnych prowadzono w oparciu o pomiary orientacji lokalnych w SEM wyposażonym w dział o emisji polowej.

Wyniki pomiarów orientacji lokalnych pokazują, że w obszarach zajmowanych przez makroskopowe pasma ścinania występuje ściśle zdefiniowana tendencja rotacji sieci krystalicznej, pomimo, że początkowe ziarna posiadały silnie zróżnicowaną orientację. Niezależnie od orientacji poszczególnych ziaren, w obszarze makroskopowych pasm ścinania ich sieć krystaliczna rotuje w taki sposób, że w każdym ziarnie jedna z płaszczyzn {111} 'zmierza' do nałożenia się z płaszczyzną maksymalnych naprężeń ścinających. Umożliwia to propagację poślizgu poprzez granice ziaren wzdłuż kierunku ścinania bez widocznej zmiany w kierunku poślizgu. Naturalną konsekwencją takiej rotacji jest uformowanie się specyficznej tekstury 'wnętrza' makroskopowych pasm ścinania.

## 1. Introduction

Shear bands (SB) or their compact clusters, called macroscopic shear bands (MSB), are frequently observed examples of unstable behavior of fcc metallic materials at large strains. However, their formation and development within the as-deformed structures and their influence on the overall texture evolution are still not completely understood.

The crystallographic aspects of shear banding in single crystals of medium-high stacking fault energy (SFE) metals

had been analyzed in the past, e.g. [1-4] and for low SFE metals, e.g. [5-10] using X-ray diffraction or local orientation measurements in TEM and SEM. It was stated that, regardless of SFE, the shear banding is preceded by the formation of obstacles to homogeneous dislocation glide in the crystallite. However, the formation of these obstacles is strongly influenced by the crystallography and SFE. Two groups of SB can be distinguished. If the obstacles are fine, twin-matrix lamellae, typical for metals with low SFE, the SBs are classified as *brass-type*. If the precursory obstacles are the elongated dislocation walls

\* POLISH ACADEMY OF SCIENCES, INSTITUTE OF METALLURGY AND MATERIALS SCIENCE, 30-059 KRAKÓW, 25 REYMONTA STR., POLAND

\*\* AGH UNIVERSITY OF SCIENCE AND TECHNOLOGY, FACULTY OF NON-FERROUS METALS, 30-059 KRAKÓW, AL. MICKIEWICZA 30, POLAND

of a cell block structure, the shear bands are of the *copper-type*. They are typically observed in materials with high or medium SFE. In both cases, the rotation-induced mechanical instability within narrow areas of the anisotropic structure of elongated cells or twin-matrix layers leads first of all to the *kink-type bands* and next to the formation of SBs [9,11].

There is still no agreement on the fundamental problem whether the slip within the SBs is crystallographic or non-crystallographic, i.e. whether glide occurs on  $\{111\}$  planes along  $\langle 110 \rangle$  directions in fcc metals. In the case of twinned structures of metals with low or middle-high SFE, there is a question how twin-oriented lamellas are incorporated into SBs, and it is not clear if SBs can modify the global deformation texture, and if they can, what is the mechanism of the modification?

The opinion that SBs are non-crystallographic derives from macroscopic observations and general considerations of the stability of the  $\{112\}\langle 111 \rangle$  orientation at high strains, as initially proposed in [12,13]. A second argument used by authors advocating non-crystallographic character of SBs, e.g. [12-14] is that the macroscopically observed shear occurs in a plane different from the  $\{111\}$  plane in the matrix (twinned or non-twinned). On the other hand, the concept of crystallographic nature of SBs is based on the assumption of their formation as a result of local lattice re-orientations, e.g. [7-9,11]. This rotation leads to kink-bands as a precursor of SBs [7], and as a consequence, to re-orientation of the  $\{111\}$  plane towards the shear plane [8,11,15]. In polycrystalline metals the situation can be quite complicated [16]. In this case macroscopic shear bands very often cross the grain boundaries without any significant change in the shear direction. From the point of view of crystallography, the requirement of slip propagation across grain boundaries leads to some basic questions about the mechanisms responsible for slip system organization along traces of the shear plane within differently oriented grains (or their fragments) situated inside the sheared zone. In this context, the main debate again centers on whether *slip within an MSB is crystallographic or non-crystallographic*.

These fundamental controversies clearly indicate that despite considerable interest in shear banding, the real elementary mechanism of SB nucleation, their development, and their contribution to the formation of rolling deformation and recrystallization textures still constitutes a set of unresolved problems.

In this work, the (micro)texture development in polycrystalline Al-0.23wt.%Zr alloy has been investigated in order to characterize the influence of local lattice re-orientations within the structure of flat feathery grains (formed under certain heat and flow conditions during unidirectional solidification) on the formation of macroscopically visible clusters of shear bands and slip propagation across grain boundaries. Computer-automated electron backscattered diffraction (EBSD) is a particularly suitable method of investigating the phenomenon.

## 2. Material and methods

The material used in this work was Al-0.23wt.%Zr alloy. After unidirectional solidification the twin boundaries between

flat, feathery grains were formed. They were situated parallel to the solidification direction. The compact clusters of twins constitute the material used to develop MSB. Samples with dimensions of  $10 \times 10 \times 10 \text{ mm}^3$  were carefully machined using a wire saw from the as-grown ingots.

The samples were cut-off in such a way that the twinning planes were situated almost parallel to the one of the sample plane. In channel-die rig the twinning planes were situated parallel to the compression plane (Fig. 1). The samples were deformed in plane strain compression at a nominal strain rate of  $10^{-4} \text{ s}^{-1}$ . The deformation was performed at 77 K by immersing the channel-die rig in liquid nitrogen. In order to reduce the frictional constraint between specimen and compression rig, a  $50 \mu\text{m}$  thick Teflon<sup>TM</sup> lubricant was used during testing. The samples were deformed up to final strains of 0.69, using multi-stage tests. At each step ( $\sim 0.2$  strain), the Teflon<sup>TM</sup> ribbon was changed, so that friction was very low. The ratio between the height and the length of the test pieces was restored to 1 at the beginning of each deformation step. A thickness reduction of about 0.69 was chosen for a detailed analysis of the influence of internal MSB substructure on slip propagation across grain boundaries and texture changes.

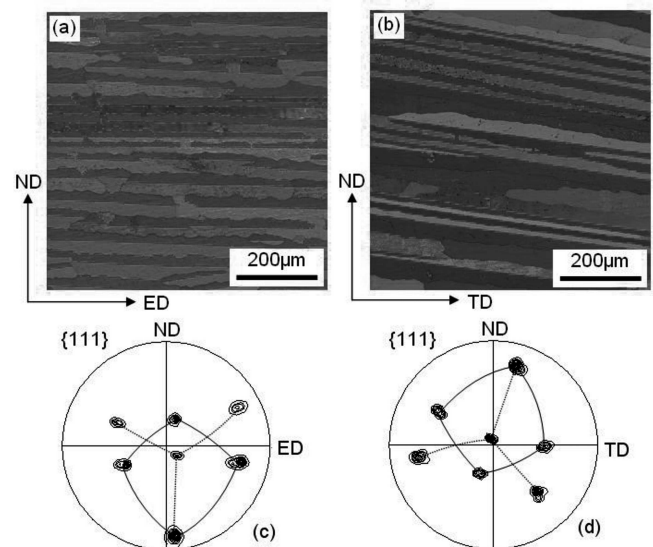


Fig. 1. Microstructure and texture of feathery grains in Al-0.23wt.% alloy after unidirectional solidification. Orientation maps and corresponding  $\{111\}$  pole figures measured in: (a) and (c) ND-ED section, (b) and (d) ND-TD section. 'All Euler' color code was applied. SEM/EBSD measurements with step size of  $2 \mu\text{m}$

Specimens for optical microscopy observations and local orientation measurements were cut from the deformed crystals perpendicular to transverse direction (TD), i.e. with edges parallel to extension (ED) and normal (ND) directions. The indices  $\{hkl\}\langle uvw \rangle$  represent the texture component that has the  $\{hkl\}$  plane parallel to the ND-ED plane and the  $\langle uvw \rangle$  direction parallel to the ND. The sample coordinate system for channel-die is presented in Figure 1.

The local changes in crystallographic orientations of initial and deformation-induced structures were investigated by SEM – QUANTA 3D FEG SEM equipped with a field emission gun (FEG) and facilities for electron backscattered diffraction (EBSD). The voltage of 20 kV, the working distance

of 10 mm, and the specimen tilt angle of 70 degrees were used. The microscope control, pattern acquisition, and indexing were done using the TSL OIM Analysis 5 software (EDAX, Inc., Mahwah, NJ). The mappings were carried out in the beam scanning mode mostly with the step size of 100 nm.

### 3. Results and discussion

#### 3.1. Initial microstructure and texture

The microstructure and texture of samples after solidification was characterized by SEMFEG/EBSD system in two sections, i.e. perpendicular to TD and ED. The orientation maps made in both sections shows that the width of flat grains varies slightly in different areas of the sample. In ND-ED section the traces of the grain boundaries were mostly parallel to ED, as presented in Fig. 1a. The thickness of particular grains ranged between 30  $\mu\text{m}$  and 60  $\mu\text{m}$ . An EBSD system identified these boundaries as twin-type. Accordingly, the texture was dominated by two twin-related components.

The boundaries between grains are situated almost parallel to the compression plane. The slight deviation is well-visualized by an additional sample characterization in ND-TD section (Fig. 1b) that shows the traces of the twinning planes to be inclined by  $\sim 10^\circ$  to TD. The microstructure observed in this section seems to be finer with respect to those observed in ND-ED ones. In that case, the width of particular grains ranged between 20  $\mu\text{m}$  and 40  $\mu\text{m}$ . The texture of the initial material was dominated by two, twin-related components, as presented on  $\{111\}$  pole figures in Figs. 1c and d. The flat, twin related grains were almost perfectly distributed inside whole volume of initial material.

#### 3.2. The matrix orientation changes. Deformation induced crystal lattice rotation

Different volumes of the sample undergo different rotation tendency. At the first approximation the rotation process can be 'described' by the inclination angle changes of the initial grain boundaries. It is important to remember that before the deformation, the traces of most of the grain boundaries observed in ND-ED section were situated parallel to ED.

The microstructures and textures of the alloy after strains of 0.36 and 0.69 in middle areas of the sample (i.e. outside the MSB) are presented in Fig. 2. The analysis of the orientation maps and corresponding  $\{111\}$  pole figures clearly shows that particular grains undergo independent rotation around selected axes. The middle areas of the sample clearly show that the traces of initial grain boundaries are still parallel to ED. However, the crystal lattice of both groups of grains undergoes significant (and differently 'directed') rotation, as compared to initial positions. The  $\{111\}$  pole figures well document the rotations around axes lying near the TD. Most of the rotation axes were close to the  $\langle 112 \rangle$  direction. This indicates that the slip systems of  $\{111\}\langle 110 \rangle$ -type, play a decisive role in the strain accommodation during the deformation. Moreover, the slip systems that decide about the observed rotation tendency of each group of grains were characterized by the highest Schmid factor.

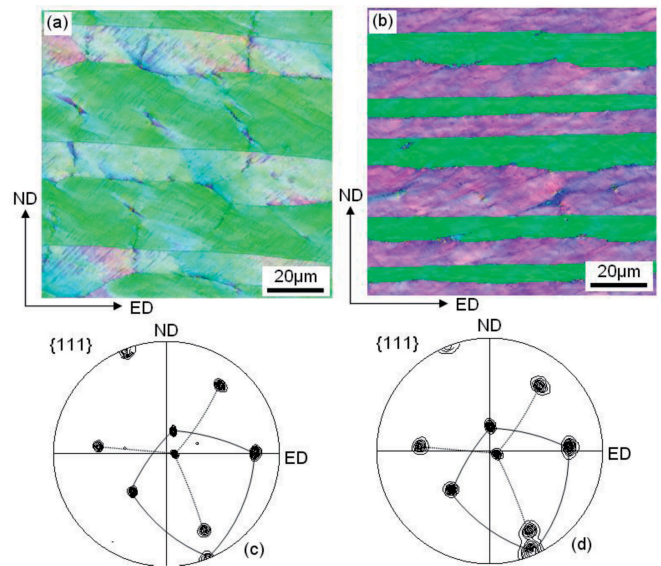


Fig. 2. Microstructure and texture of feathery grains in middle area of the deformed samples. Orientation maps and corresponding  $\{111\}$  pole figures after: (a) and (c) 0.36 strain, (b) and (d) 0.69 strain. 'IPF ( $\parallel Y$ )' color code was applied. SEM/EBSD measurements with step size of 100 nm. ND-ED section

The analysis of the grain boundaries shows that the boundaries separating the grains periodically lose and regain twinned character due to strain induced rotation. After strains of 0.36 and 0.69 in the middle areas of the sample (Figs. 2a and b) the grain boundaries do not fulfill twin-relation (Brandon criterion). This clearly indicates that within differently oriented grains the dominating slip systems lead to different rotation tendencies. Additionally, after higher strains the areas saturated by sub-grain boundaries occupy a significant part of the crystallites. As a result the substructure is finer than that observed in the initial state and after the strains of 0.36. The thickness of flat grains, i.e. the distance between grain boundaries along ND, decreases to about 10-20  $\mu\text{m}$  after strains of 0.36 and below 10  $\mu\text{m}$  after strains of 0.69.

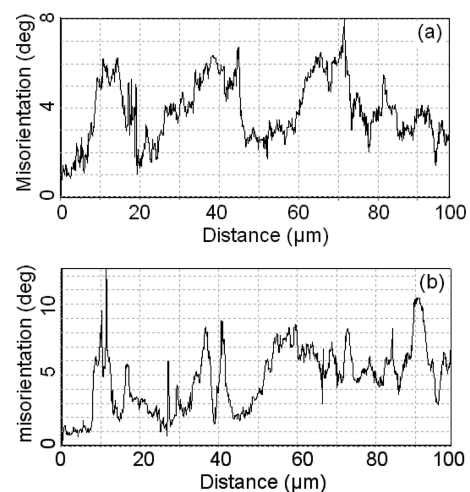


Fig. 3. Misorientation profile along line scan parallel to ED after strain of (a) 0.36 and (b) 0.69. Middle areas of the samples. SEM/EBSD measurements with step size of 100nm. ND-ED section

In the middle area of the sample for the range of deformations below 0.69 the misorientation angle of misorienta-

tion relations between the grains attains values between  $10^\circ$  and  $15^\circ$  (Fig. 3), and the misorientation axes are close to a  $\langle 112 \rangle$  direction. Within particular grains no significant differences in the distribution of misorientations were observed, as presented in Fig. 3a and b showing two lines scan along ED.

### 3.3. Shear bands formation – macroscopic analysis

The samples did not deform homogeneously in the channel-die. The most characteristic feature of the deformation microstructure is the formation of band-like heterogeneities of deformation in the form of shear bands. The shear bands and their compact clusters called macroscopic shear bands are revealed by optical microscopy in the anodized ND-ED plane. At lower deformations (strain below 0.36) the substructure is composed of relatively broad (and only slightly marked) bands inclined at  $\sim 45^\circ$  to ED (Fig. 4a). They penetrate the whole volume of the sample in plane parallel to TD and show a clearly marked tendency to intersect the grain boundaries.

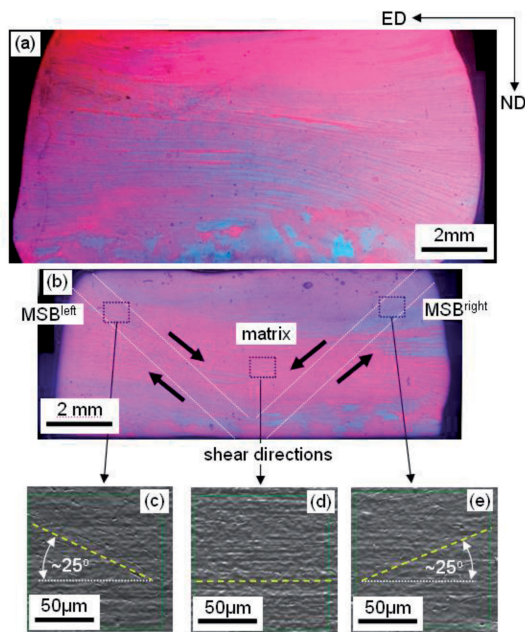


Fig. 4. Macroscopic shear bands formation in sample after strain of: (a) 0.36 and (b) 0.69. Details of the microstructure observed in secondary electrons in SEM, in areas of: (c) –  $MSB^{left}$ , (d) – matrix between  $MSB$  and (e) –  $MSB^{right}$ . Optical microscopy and SEM imaging in secondary electrons

As a result of this intersection a pronounced displacement of the grain boundary fragments and their rotation is prominent. After the strains of 0.69, the differences were observed in the intensity of plastic flow due to successive strain localizations within MSBs. The MSBs practically fill the whole thickness of the sample and form a characteristic V shaped set of two families (Fig. 4b). The width of each set was 0.8-1.0mm and they were positively and negatively inclined at  $\sim 45^\circ$  to ED. The grain boundaries observed on the longitudinal plane showed a well-defined rotation (Figs. 4c-e) of opposite sign within each set of bands. This rotation occurs with the increasing inclination of the boundary segments crossed by MSBs. The values of the rotation angles inside  $MSB^{left}$  and  $MSB^{right}$  attain  $\sim \pm 20-25^\circ$  (Figs. 4c and e). The inclination of the traces of grain boundaries decreases outside the bands.

The MSBs are composed of (micro-)shear bands, as previously observed in low SFE metals, e.g. [7, 11]. These (micro-)shear bands are clearly inclined by about  $\pm 40-45^\circ$  with respect to ED. They run across the whole thickness of the crystal and show only slightly different inclinations with respect to ED. Within the MSBs, most of the substructure of particular grains is occupied by areas with a high density of dislocation sub-boundary arrays and separated by thin areas with a low density of misoriented sub-boundaries, as observed in Ag [9] and Fe [17]. The traces of the (micro-)shear bands were more intensively grouped close to both top corners of the sample. The intensity of shearing within MSB decreases in areas near the bottom surface.

A more detailed analysis within selected areas made by means of SEM/BSE imaging (in the same section) clearly confirms the tendency of opposite sign crystal lattice rotation within symmetrically situated MSBs (Figs. 4c-e). At the first approximation within narrow areas of the shear bands the traces of grain boundaries rotate around TD towards the shear planes.

### 3.4. Slip propagation across grain boundaries and MSB induced textural changes

The analysis of crystal lattice rotations in particular grains was based on local orientation measurements. This part of the analysis was dedicated to explanation of the mechanisms responsible for the slip propagation across grain boundaries. After strains of 0.69 two sets of MSBs located symmetrically with respect to the plane perpendicular to ED extending over the entire sample thickness. These broad MSBs observed in the plane perpendicular to TD are made of compact packets or bundles of SBs.

Figures 5a and b show the EBSD maps made in the regions of the localized shear in the sample compressed up to strains of 0.69. More or less parallel (micro-)shear bands are the important ‘components’ of the deformation microstructure in the area of MSB. In all analyzed grains a tendency to grain subdivision and a strong strain-induced re-orientation was observed. From the point of view crystallography, the areas of MSB were characterized by a crystallographic orientation different from the surrounding matrix (for comparison see Fig. 2).

In the case of both sets of MSB the microtextures of whole orientation maps shows the formation of two, nearly complementary  $S\{123\}\langle 634 \rangle$  orientations. It is visible that the crystal lattice inside the particular MSB rotates around axes lying close to TD in opposite ‘directions’. This specific crystallographic texture development, observed at increasing deformation, favors the penetration of slip in the MSB area through the neighboring grains along planes inclined at  $\sim 45^\circ$  to ED. The crystal lattice rotated in such a way that one of the  $\{111\}$  slip planes became nearly parallel to the plane of the maximum shear. A natural consequence of this rotation is the formation of a specific MSB microtexture which facilitates the slip propagation across grain boundaries along the shear direction without any visible variation in the slip direction, as observed earlier in polycrystalline copper [16].

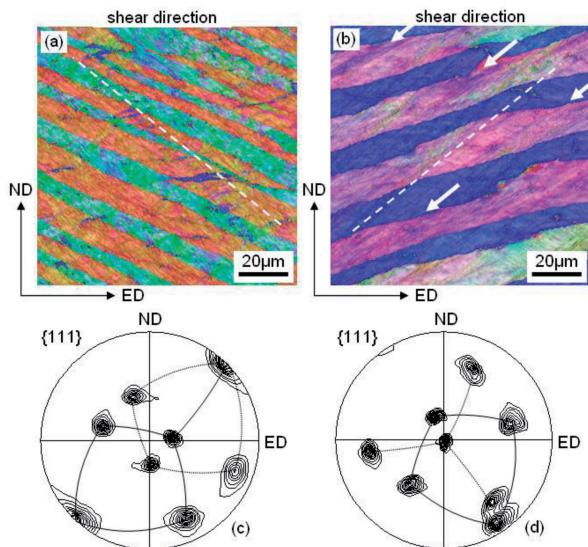


Fig. 5. Microstructural and textural changes in areas of macroscopic shear bands showing opposite tendency of crystal lattice rotation. Orientation maps and corresponding  $\{111\}$  pole figures in areas of: (a) and (c) –  $MSB^{left}$ , (b) and (d) –  $MSB^{right}$ . SEM/EBSD measurements with step size of 100 nm. ND-ED section. 'IPF ( $\parallel Y$ )' color code was applied

Figures 6 and 7 show the more detailed orientation maps taken within the deformed microstructure of an MSB. Since the grain boundaries are crossed by (micro-)shear bands, characteristic steps are formed on the boundary. This indicates large shear strains due to localized slip associated with (micro-)shear bands. The orientations of grains are shown in attached  $\{111\}$  pole figures. It is again clearly marked that the crystal lattice of particular grains rotated in such a way that one of the  $\{111\}$  slip planes became nearly parallel to the plane of maximum shear although the orientations of neighboring grains were quite different. Additionally, in each case one of the  $\langle 011 \rangle$  or  $\langle 112 \rangle$  – type directions, lying in these planes, systematically tended to coincide with shear direction.

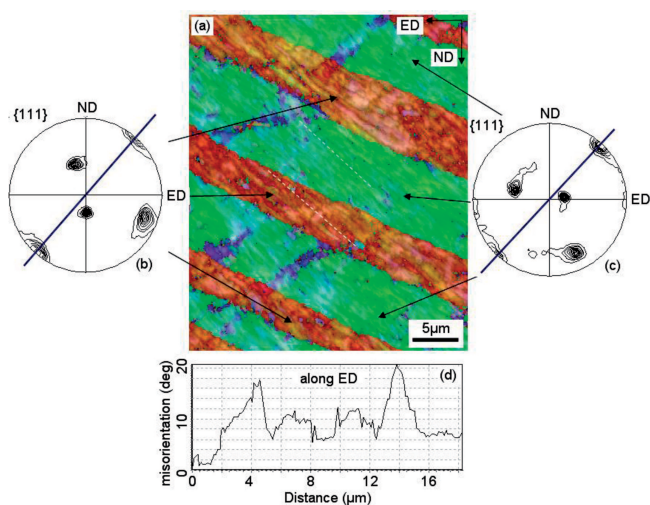


Fig. 6. Details of microstructural and textural changes in the areas of  $MSB^{left}$ . (a) Orientation map, and (b) and (c) the  $\{111\}$  pole figures showing textures of particular grains. (d) Misorientation line scan along ED, typically observed in both groups of grains. SEM/EBSD measurements with step size of 100 nm. ND-ED section. 'IPF ( $\parallel Y$ )' color code was applied

This leads to the important conclusion that the macroscopically observed shear plane in fact consists of small parts limited to particular grains (or their fragments). These parts were only slightly deviated from the macroscopic shear plane. It is important also to note that the higher the strain, the smaller the deviations from the macroscopically observed shear plane.

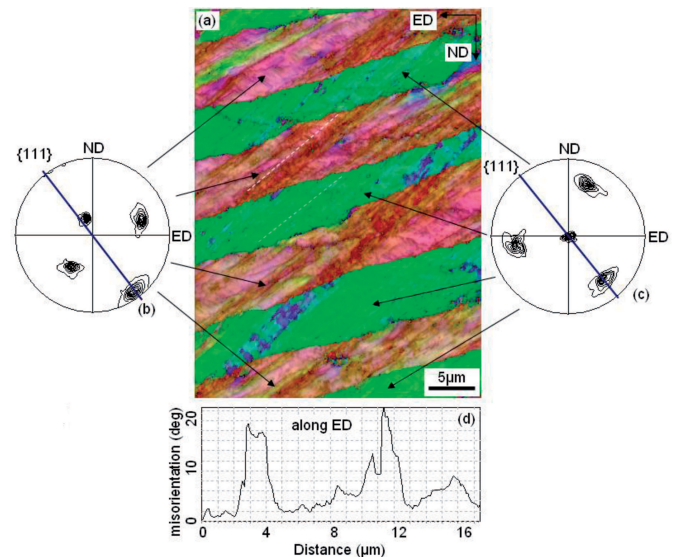


Fig. 7. Details of microstructural and textural changes in the areas of  $MSB^{right}$ . (a) Orientation map, and (b) and (c) the  $\{111\}$  pole figures showing textures of particular grains. (d) Misorientation line scan along ED, typically observed in both groups of grains. SEM/EBSD measurements with step size of 100 nm. ND-ED section. 'IPF ( $\parallel Z$ )' color code was applied

The accumulation of (micro-)shear bands into bundles and their propagation through grain boundaries is an important problem in the process of MSB formation in polycrystalline metals. The situation is simple when neighboring grains have a similar orientation, and the  $\{111\}$  planes coincide with the plane of maximum shear stress; depending on the state of anisotropy the shear plane is inclined usually at  $35\text{--}45^\circ$  to ED ( $45^\circ$  for isotropic material). Slip penetration, however, occurs in regions of quite different orientations. Nevertheless, *from the crystallographic point of view, the existence of a common  $\{111\}$  plane for both areas is required; it is along this plane that slip can penetrate the boundary.* This was clearly visible within the grains lying inside the MSB. Along the grains, the crystal orientation changed periodically and the accumulated point-to-origin misorientations varied by  $20\text{--}25^\circ$  (Figs. 6d and 7d) but their axes were close to one of the  $\langle 112 \rangle$  or  $\langle 110 \rangle$  poles.

#### 4. Conclusions

Microtexture measurements on polycrystalline Al-0.23%Zr alloy compressed in the channel-die have been used to analyse the propagation of macroscopic shear bands. They showed that well-defined crystal lattice re-orientations occurred in segments of grains situated within the area of the broad MSB, although neighboring grains initially had quite different crystallographic orientations.

Their crystal lattice rotated in such a way that one of the {111} slip planes became nearly parallel to the direction of maximum shear. A natural consequence of this rotation is the formation of specific MSB microtextures which facilitates slip propagation across grain boundaries along the shear plane without any visible variation in the slip direction. It was thereby established that shear banding occurred across grain boundaries by the continuity of slip direction although the slip plane did not coincide exactly (in some cases) in the adjacent grains.

## REFERENCES

- [1] P. Wagner, O. Engler, K. Lücke, Formation of Cu-type shear bands and their influence on deformation and texture of rolled f.c.c. {112}<111> single crystals, *Acta Metall. Mater.* **43**, 3799-3812 (1995).
- [2] H. Inagaki, M. Koizumi, C.S.T. Chang, B.J. Duggan, Orientation imaging microscopy of the shear bands formed in Al-5%Mg alloys during cold rolling, *Mater. Sci. Forum* **587-592**, 396-402 (2002).
- [3] A. Huot, R.A. Schwarzer, J.H. Driver, Texture of shear bands in Al-Mg3% (AA5182) measured by BKD, *Mat. Sci. Forum* **273-275**, 319-326 (1998).
- [4] H. Paul, M. Darrieulat, A. Piątkowski, Local Orientation Changes and Shear Banding in {112}<111>-Oriented Aluminium Single Crystals, *Z. Metallkd.* **92**, 1213-1221 (2001).
- [5] A. Weider, P. Klimanek, Shear banding and texture development in cold rolled  $\alpha$ -brass, *Scripta Materialia* **38**, 851-856 (1998).
- [6] E. El-Danaf, S.R. Kalidindi, R.D. Doherty, C. Necker, Deformation texture transition in  $\alpha$ -brass: critical role of micro-scale shear bands, *Acta Materialia* **48**, 2665-2673 (2000).
- [7] H. Paul, J.H. Driver, C. Maurice, Z. Jasieński, The Structure of Shear Bands in Twinned FCC Single Crystals, *Mat. Sci. Engn.* **A359**, 178-191 (2003).
- [8] H. Paul, A. Morawiec, E. Bouzy, J.J. Fundenberger, A. Piątkowski, Orientation Imaging in scanning electron and transmission electron microscopy for characterization of shear banding phenomenon, *Microchimica Acta* **155**, 243-250 (2006).
- [9] H. Paul, J.H. Driver, C. Maurice, A. Piątkowski, The role of shear banding on deformation texture in low stacking fault energy metals as characterized on model Ag crystals, *Acta Materialia* **55**, 833-847 (2007).
- [10] C.S. Da Costa Viana, J.C. Parades, A.L. Pinto, A.M. Lopez, EBSD analysis of shear banding in  $\alpha$ -brass, in: J. Szipunar (Ed.), *Proceeding of the 12th International Conference on Textures of Materials*, Trans. Tech. Publ., Toronto, Canada, 671-676 (1999).
- [11] H. Paul, A. Morawiec, J.H. Driver, E. Bouzy, On twinning and shear banding in a Cu-8at.%Al alloy plane strain compressed at 77K, *International Journal of Plasticity* **25**, 1588-1608 (2009).
- [12] Y. Nakayama, K. Morii, Transmission electron microscopy of shear band formation in rolled copper single crystals, *Transactions of the Japan Institute* **23**, 422-431 (1982).
- [13] K. Morii, H. Mecking, Y. Nakayama, Development of shear bands in fcc single crystals, *Acta metallurgica* **33**, 379-386 (1985).
- [14] A. Korbel, P. Martin, Microscopic versus macroscopic aspect of shear bands deformation, *Acta materialia* **34**, 1905-1909 (1986).
- [15] H. Paul, J.H. Driver, Deformation behaviour of channel-die compressed Al bicrystals with {100}<001>/{110}<011> orientation, *Archives of Metallurgy & Materials* **50**, 209-218 (2005).
- [16] H. Paul, J.H. Driver, The influence of shear bands on microtexture evolution in polycrystalline copper, *Application of Texture Analysis: Ceramic Transactions* **201**, 181-188 (2008).
- [17] D. Dörner, Y. Adachi, K. Tsuzaki, Periodic crystal lattice rotation in microband groups in a bcc metal, *Scripta Materialia* **57**, 775-778 (2007).

Received: 20 April 2012.